Analysis of instability in an industrial ammonia reactor

John C. Morud   Sigurd Skogestad[*]

Chemical Engineering, Norwegian Univ. of Science and Technology (NTNU)

N-7034 Trondheim, Norway

January 6, 1998

Abstract

The starting point for this study was an incident in an industrial plant, where the ammonia synthesis reactor became unstable with rapid temperature oscillations (limit cycles) in the range from about $300^{o}C$ to $500^{o}C$. A simple dynamic model reproduces this behavior. In industry a steady-state Van Heerden analysis is often used to analyze the stability, but a more careful analysis for this reactor system reveals that instability occurs when there still is positive steady-state margin, namely as a pair of complex conjugate poles cross the imaginary axis (Hopf bifurcation). This is consistent with the observations where the instability manifests itself as oscillations rather than extinction of the reaction. This somewhat unusual behavior can be explained by the presence of an inverse response for the temperature response through the reactor beds combined with the positive feedback caused by the preheater.

[*]Author to whom correspondence should be addressed. E-mail: skoge@chembio.ntnu.no, Phone: 47-7359-4154, Fax: 47-7359-4080.

1   Introduction

The starting point of this work was an incident in an industrial ammonia fixed bed synthesis reactor in Germany in 1989. After a sudden decrease in reactor pressure caused by a temporary reduction in fresh feed to the synthesis loop, the reactor – which was operated without feedback control – became unstable, such that the recorded temperatures in the reactor started oscillating with a period of about 6 minutes and a range of about 200 $^{\circ}C$ ($\pm 100^{\circ}C$) (Naess *et al.*, 1992). The oscillations lasted for about two hours, until pressure in the synthesis loop was restored. A temperature recording from this incident is shown in Figure 1. Such large and rapid oscillations are damaging for the catalyst, and after the incident it was observed that this kind of oscillations tended to occur more frequently and for smaller disturbances.
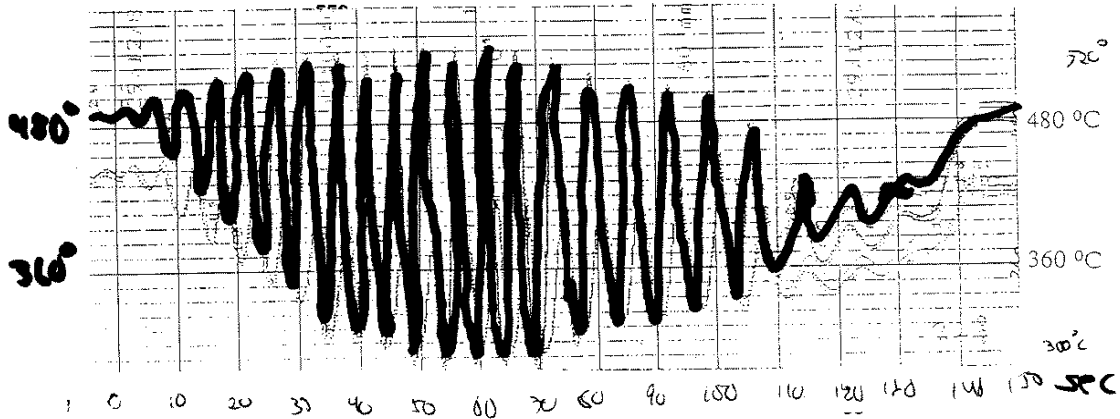

Figure 1: Temperature recording from the industrial ammonia reactor (close to the reactor outlet). (NOTE: Time scale is 0 to 150 MINUTES)

The purpose of this paper is to provide an explanation of this sort of reactor behavior. First, we present a mathematical model of the ammonia synthesis reactor – describing the conservation of mass and energy. Simulations using this model reproduce the temperature oscillations observed in the industrial plant. The main cause of the instability is the positive feedback from the heat recycle caused by the feed-effluent heat exchanger. We first start with a simple steady-state analysis, similar to that of van Heerden (1953), which proves to be inadequate. We then perform a conventional linear stability analysis, which is found to be consistent with the nonlinear simulations and shows that instability occurs as a pair of complex eigenvalues cross into the right half plane (Hopf bifurcation). We explain why the initial steady-state analysis was inadequate in this case. Finally, we discuss the implications for operation and control of such reactors.

Although it is well-known that instability of this kind may occur in chemical reactors, this is to our knowledge the first time it is documented on an industrial scale. Also, the paper demonstrates the usefulness of classical frequency-domain analysis such

2

as Nyquist and Bode plots, and shows in which cases the steady-state analysis of van Heerden may be incorrect.

The rest of this introduction is devoted to a short review of previous work. General work on reactor stability, modeling and control is abundant. Crider and Foss (1968) refer to Nusselt in 1927 and independently Schuman in 1929 as the first to present a thermal analysis of packed beds. Van Heerden (1953) and Aris and Amundson (1958) analyzed the stability of the steady states of autothermal reactors. Limit cycle behavior in autothermal reactors was presented by Reilly and Schmitz (1966,1967) and Pareja and Reilly (1969). Stephens and Richards (1973) performed a steady state and dynamic analysis of an ammonia synthesis plant and noted that steady state stability criteria are not sufficient for stability. Fixed bed reactors are discussed extensively in the survey of Schmitz (1975), and also in Ray (1972), Eigenberger (1976, 1985) and Jørgensen (1986). Silverstein and Shinnar (1982) discuss the stability of heat integrated fixed bed reactor. Other works on dynamics and control of fixed bed reactors include Crider and Foss (1966, 1968) Vakil *et al.* (1973), Wallmann and Foss (1979, 1981), Foss *et al.* (1980), Gusciora and Foss (1989), and Eigenberger and Schuler (1989).

2   A simple model of the reactor

Models for fixed beds are abundant in the literature (see e.g. Eigenberger, 1976). The main purpose of our model is **not** to reproduce the industrial case with great numerical accuracy, but rather to yield qualitative insight into the observed phenomenon. Our model is therefore kept simple.

Figure 2 shows a sketch of the reactor system, consisting of three beds in series with fresh feed quenching between each beds and preheating of the feed with the effluent. A material and energy balance yield two partial differential equations:

$$w\frac{\partial c}{\partial z} = m_c r(T, c) \tag{1}$$

$$m_c C_{pc}\frac{\partial T}{\partial t} + w C_{pg}\frac{\partial T}{\partial z} = (-\Delta H_{rx})m_c r(T, c) + , m_c C_{pc}\frac{\partial^2 T}{\partial z^2} \tag{2}$$

where:

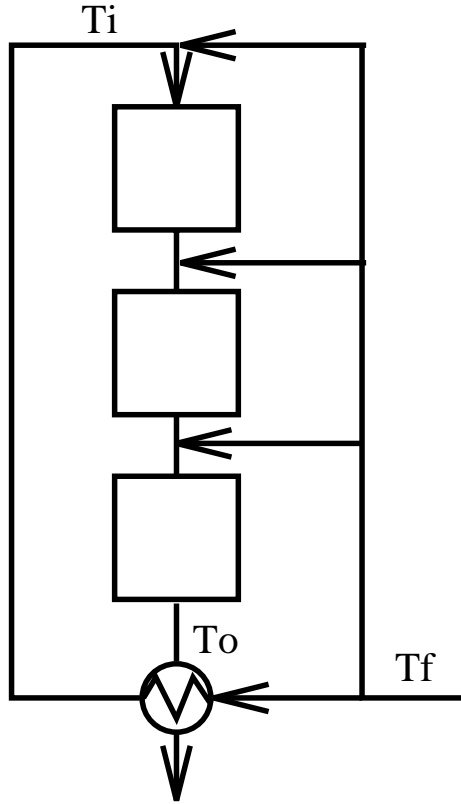|		
t	Time	[sec.]
z	Position in reactor	[-]
T	Catalyst particle temperature	[K]
c	Ammonia concentration (mass fraction)	[kg NH3/kg gas]
ΔH_{rx}	Heat of reaction	[J/kg.NH3]
C_{pc}	Heat capacity of catalyst	[J/kg cat, K]
C_{pg}	Heat capacity of gas	[J/kg, K]
m_c	Catalyst mass in the bed	[kg]
w	Gas flow through the bed	[kg/s]
$r(T, c)$	Reaction rate	[kg NH3/kg cat, s]
,	Dispersion coefficient	[1/s]

Figure 2: Sketch of reactor system with three beds and preheater.

Note that gas phase holdup has been neglected because the gas density is low. The dispersion coefficient is a simplified way of taking into account the finite heat transfer rate between the gas phase and the solid catalyst.

The model may be discretized in space, and by selecting the grid spacing $\Delta z = 2, /u$ the term involving the diffusion drops out (effectively, the numerical "diffusion" introduced by the discretization cancels the actual diffusion). We then get the following discretized equations for cell no. j (see Morud (1995) for more details):

$$0 = w(c_{j-1} - c_j) + m_{c,j} r(T_j, c_j) \tag{3}$$

$$m_{c,j} C_{pc} \frac{dT_i}{dt} = w C_{pg}(T_{j-1} - T_j) + m_{c,j} r(T_j, c_j)(-\Delta H_{rx}) \tag{4}$$

(Alternatively, this is a valid model for cases where the diffusion is neglected and the number of grid points is large.)

An important parameter for the reactor is the migration velocity for the temperature wave,

$$u = \frac{w C_{pg}}{m_c C_{pc}} \tag{5}$$

With the data used in the simulations the migration velocity through each of the three beds is 0.0111, 0.0092 and 0.0067 [bed lengths/s], respectively. The total time

4

for a temperature wave to move through the the three beds is then approximately $1/u_1 + 1/u_2 + 1/u_3 = 348$ s.

The preheater is modeled as a as a standard countercurrent heat exchanger (without dynamics for simplicity) which yields a relationship of the form:

$$T_i = \epsilon T_o + (1 - \epsilon)T_f \tag{6}$$

where T_i is the preheater outlet (reactor inlet) temperature and T_o the reactor outlet temperature (see Figure 2), and the preheater efficiency $\epsilon \in [0 \quad 1]$ is a constant independent of temperature.

The reaction rate for the reaction $N_2 + 3H_2 \rightleftharpoons 2NH_3$ is computed from the Temkin-Pyzhev equation (as given by Froment and Bischoff, 1990, p. 433):

$$r_{N_2} = \frac{1}{\rho_{cat}} \cdot \left(k_1 \, p_{N_2} \cdot \frac{p_{H_2}^{1.5}}{p_{NH_3}} - k_{-1} \frac{p_{NH_3}}{p_{H_2}^{1.5}} \right) \quad [\text{kmol } N_2/\text{kg cat, h}] \tag{7}$$

where p_i denotes the partial pressure of component i [in bar],

$$k_1^o = 1.79 \times 10^4 \exp\left(-\frac{87\,090}{RT}\right) \tag{8}$$

$$k_{-1}^o = 2.57 \times 10^{16} \exp\left(-\frac{198\,464}{RT}\right). \tag{9}$$

and $r = r_{N_2} \cdot 2 \cdot 17/\rho_{cat}$ [kg NH$_3$/ kg cat, h].

However, in order to match the industrial data in Figure 1, the reaction rate was multiplied by a factor $f = 4.75$, i.e. $k_1 = f \, k_1^o$ and $k_{-1} = f \, k_{-1}^o$. The coefficient f may take into account the higher activity of the newer industrial catalyst compared to the pre-1940 catalyst used by Temkin and Pyzhev.

The Appendix contains the numerical parameter values used in the simulations. More details about the model and the approximations is given by Morud (1995). Morud found that very similar results were obtained with a model where also the heat transfer between gas and solid was included. Morud also used a more detailed kinetic model, but the results are quite similar .

3 Simulations of limit cycle behavior

Dynamic simulations using the nonlinear model reproduce the observed temperature oscillations in the industrial plant. A simulation result is shown in Figure 3, showing the reactor outlet temperature as a function of time as we make changes in the reactor pressure. Initially, the reactor operates at steady-state with a pressure of 200 bar. At $t = 0$ the pressure is reduced from 200 to 170 bar; the system remains stable (at least seemingly) and settles at a new steady-state with a somewhat lower outlet temperature. Then, at $t = 20$ minutes, we further decrease the pressure from 170 to 150 bar, and the system becomes unstable and exhibits limit cycle behavior (oscillations) very similar to those observed in the industrial reactor. At $t = 120$ min we restore the pressure from 150 to 200 bar, and the system recovers to its original steady-state.

In the above simulation we just looked at the temperature at a fixed position – the reactor outlet – as a function of time. To understand qualitatively what happens in the reactor, we now consider temperature profiles through the reactor at fixed times. Figures 4a to 4f show several such temperature profiles during one period of the sustained oscillations (taken from simulation time 103 to 109 min in Figure 3). The period of oscillations is about 7 min (420 seconds). On the horizontal axis, $z = 0$ corresponds to the inlet of the first bed and $z = 3$ to the outlet of the last bed. On the vertical axis is the reactor temperature (range 250 ^oC to 550 ^oC). The discontinuities in the figures are due to the quenching.

One should note the wavelike bump to the left in the plot in Figure 4a. 70 seconds later, see Figure 4b, the bump has moved a little to the right, growing in size. The wave may be traced through Figures 4c-f, where it induces a new wave by heat exchange with the reactor feed, resulting in the sustained temperature oscillations.

In the above simulations the feed temperature was kept constant at 250^oC, and the limit cycle behavior was induced by lowering the pressure (to less than about 170 bar). Lowering the temperature has a similar effect; with the pressure fixed at 200 bar we get instability (limit cycle behavior) when the feed temperature, T_f, is reduced from 250^oC to about 235^oC.

4   Steady-state analysis

Consider Figure 5, where the steady state characteristics of the reactor and preheater are shown. The S-shaped reactor characteristic gives the relation between the reactor
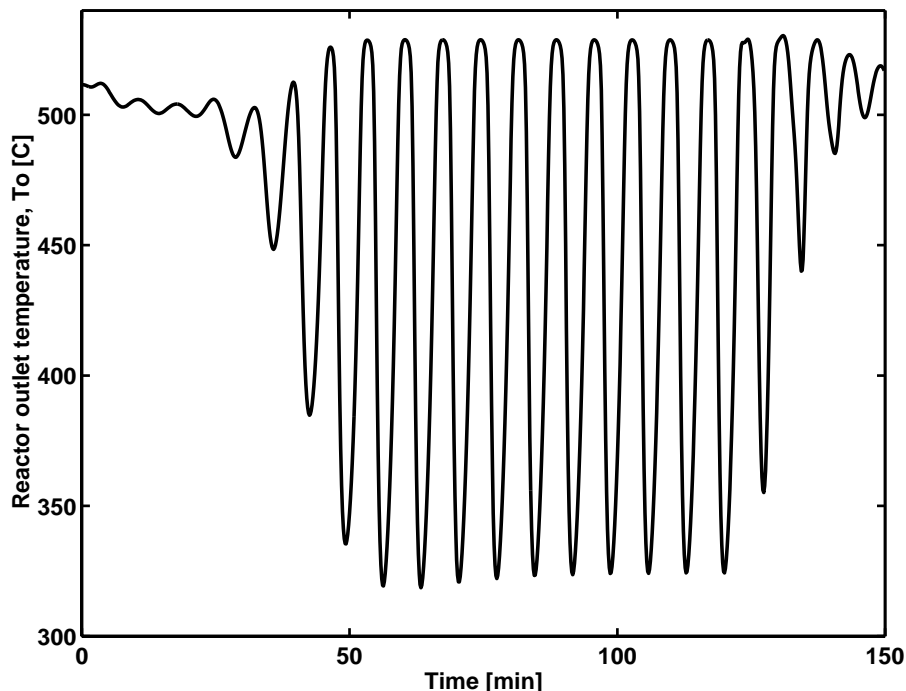

Figure 3: Nonlinear simulation of a decrease in the reactor pressure from 200 bar to 170 bar ($t = 0$), to 150 bar ($t = 20$), and back to 200 bar ($t = 120$).
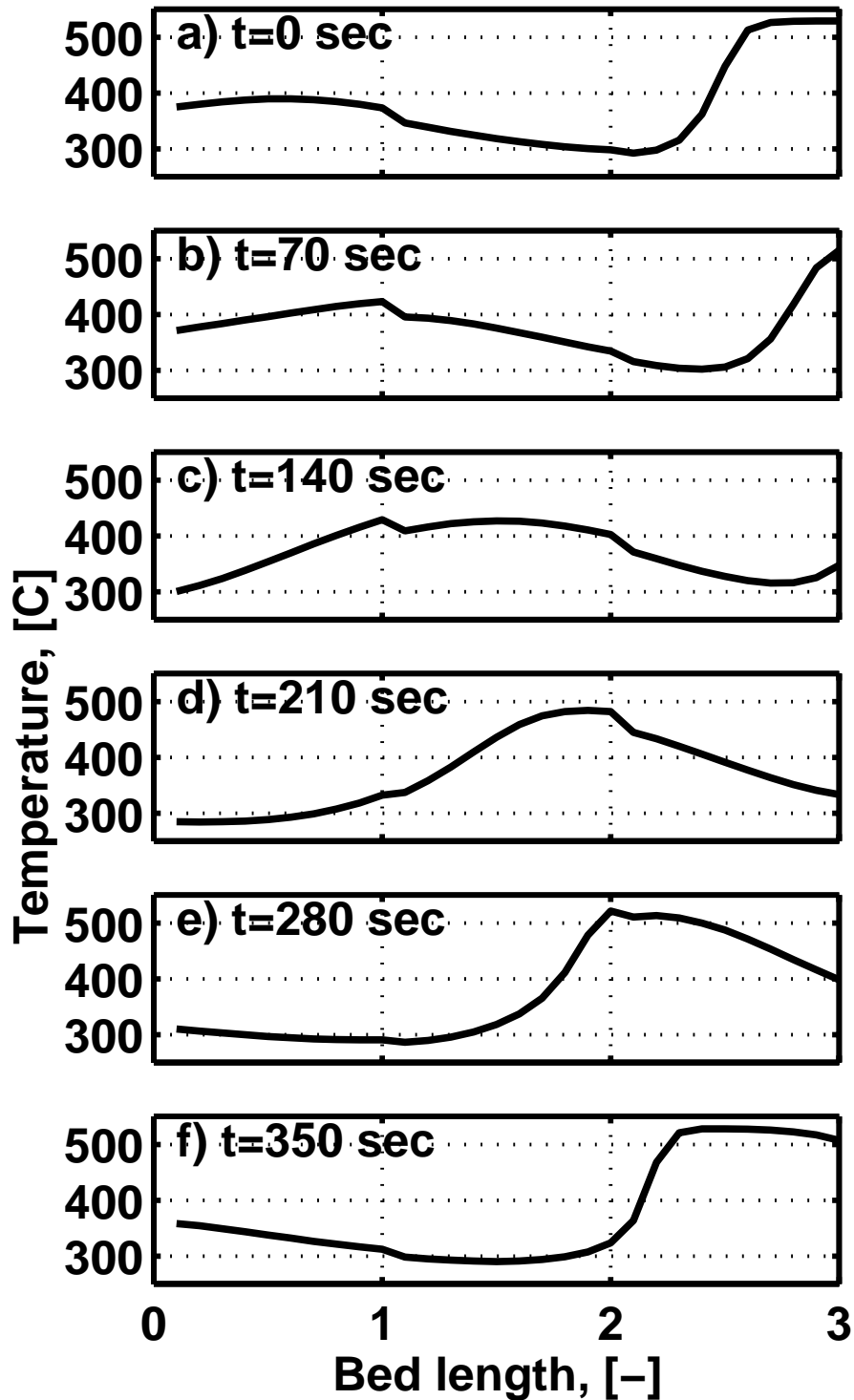
6

Figure 4: Sustained oscillations in temperature (p=150 bar).

inlet temperature T_i and the reactor outlet temperature T_o (see Figure 2 for defini-
tions). Similarly, the straight-line preheater characteristic gives the relation between
its "input" T_o and its "output" T_i, recall (6). For the reactor we show the S-shaped
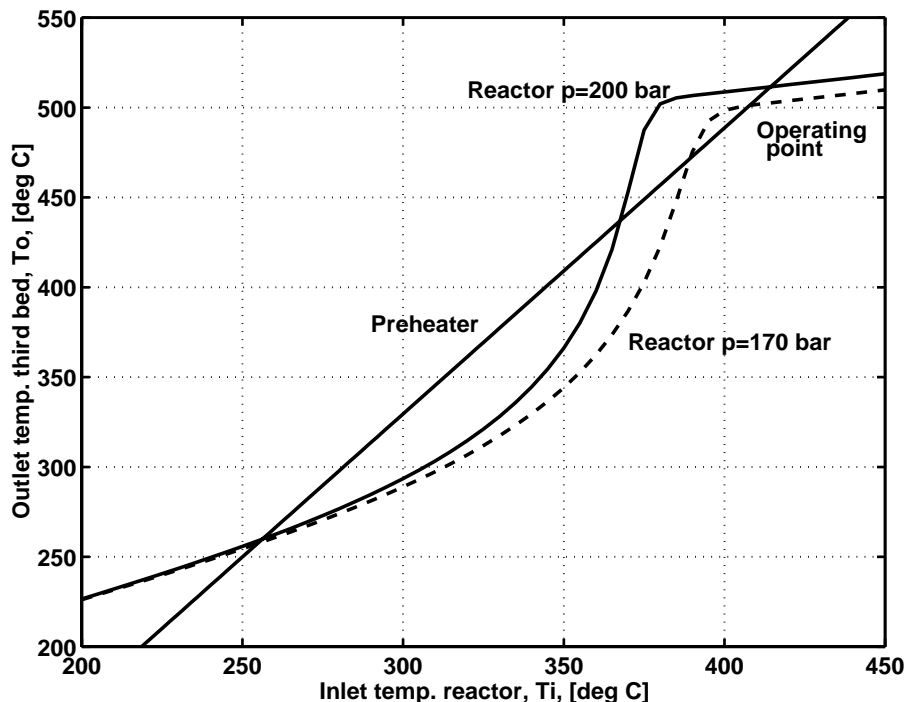
Figure 5: Steady state characteristics of reactor (S-shaped curves) and preheater (straight line).

curves at two pressures; at 200 bar (solid line) and at 170 bar (dashed line). It is implicitly assumed that other quantities are held constant (flow rates, feed temperature etc.). The plot in Figure 5 is very similar to the classical van Heerden plot (1953).

The possible steady state operating points are points where the two curves intersect. For the conditions given in Figure 5, there are three possible steady-state solutions, and the desired one, in which we operate, is the upper one with the highest temperature and highest conversion. The temperature profile through the reactor at this desired operating point is shown in Figure 6 for the two pressures. Note that the temperature at bed length zero is less than T_i because of the quench; see also Figure 2.

We now consider the stability of the desired upper operating point. As noted above, to induce instability one may reduce the pressure. According to the analysis of Van Heerden (1953), which is repeated in many books (e.g. Froment and Bischoff, 1990. p. 427), one would expect instability to occur exactly when the two characteristics in Figure 5 touch each other (i.e. when the middle and upper solutions coincide). Thus, one would expect the reactor to remain stable when the pressure is lowered from 200 to 170 bar and even a bit further down. However, simulations show that instability occurs at about 172 bar, where there still is a positive steady-state "stability margin". At first, this was believed to be caused by nonlinearity or numerical errors, but a more careful analysis shows that the simulations are indeed correct, and that the upper solution may be unstable, demonstrating that a steady-state analysis is insufficient (as pointed out already by Aris and Amundson, 1958).
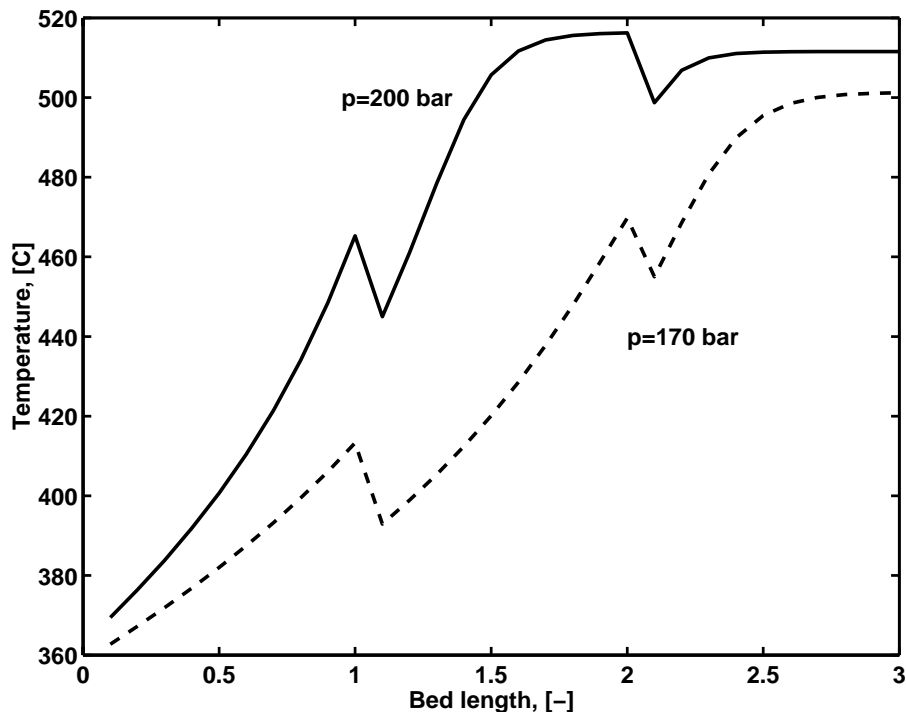
Figure 6: Steady-state reactor temperature profile at the "upper" operating point.

More specifically, we find by linearizing the model at the (upper) operating point in Figure 5 that the eigenvalues λ furthest to the right (closest to instability) are

$$p = 200 \text{ bar}: \quad \lambda = -0.0017 \pm i0.0183 \ [s^{-1}]$$

$$p = 170 \text{ bar}: \quad \lambda = +0.0002 \pm i0.0148 \ [s^{-1}]$$

Thus, the upper operating point is stable at 200 bar, but (barely) unstable at 170 bar. We note that the instability occurs as a pair of complex eigenvalues cross into the right half plane (Hopf bifurcation). The corresponding period of oscillations is approximately $2\pi/0.0148 = 425$ s which agrees very well with the observed period of oscillations of about 420 s in the nonlinear simulations and 360 s in the plant data.

5 Linear dynamic analysis

All the results given below are for a reactor with pressure 172 bar operating at the upper (desired) operating point.

Close to an operating point, the dynamics of a system is well described by its linearized model. The model of the reactor (without the preheater) was linearized numerically at this operating point, yielding a standard linear state space model with 30 states on the form:

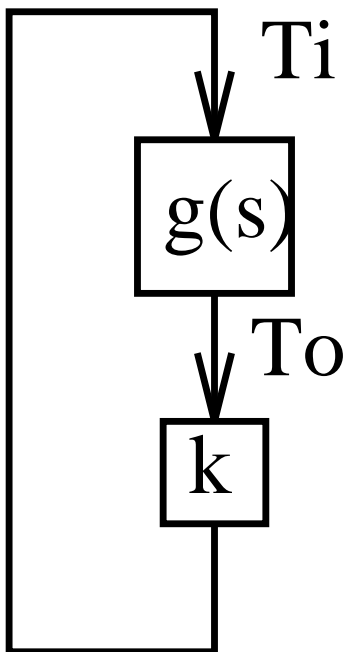$$\frac{dx}{dt} = Ax + Bu, \quad y = Cx \tag{10}$$

9

Figure 7: Block diagram of reactor (g) and preheater (k).

where the state vector x consists of temperatures along the bed; the independent variable u is the inlet temperature to the first bed, T_i (before the quench; the quench gas temperature T_f is assumed constant); and y is the outlet temperature of the third bed, T_o. We then get the input-output model

$$\Delta T_o = g(s)\Delta T_i; \quad g(s) = C(sI - A)^{-1}B$$

where the transfer function $g(s)$ is for the reactor without the preheater, and the Δ represents deviations from the nominal steady state. Linearization of the preheater model (6) gives $\Delta T_i = \varepsilon \Delta T_o$, where ε is the heat exchanger efficiency, which nominally is $\varepsilon = 0.629$. The reactor system in Figure 2 may hence be represented by the block diagram with positive feedback shown in Figure 7, where $k = \varepsilon$ is the steady state gain of the preheater and $g(s)$ the transfer function of the reactor.

Below we consider first a root locus analysis to understand what happens as we vary the feedback gain k. The results confirm that the operating point with $p = 172$ bar is at the limit to instability. Next, we perform a frequency domain analysis (Nyquist and Bode plots), which are particularly revealing, as it yields added insight into the physical cause of the instability.

5.1   Root locus analysis

The reactor with no preheater ($k = 0$) is stable. This can be seen computing the poles of $g(s)$. Thus the instability is caused by the preheating, and the eigenvalues of the "closed-loop" reactor system (with preheat) are given as the solutions to $1 - g(s)k = 0$.

10

In a root locus analysis, see Figure 8, we plot these eigenvalues (poles) as k increases from 0 to infinity (strictly speaking, k cannot exceed 1 since this corresponds to a preheater with infinite area, but we will let k exceed this value for completeness). The closed-loop poles "start" (for $k = 0$) at the poles of $g(s)$. These are marked with the symbol 'x' on the Nyquist plot, and we see that they lie quite evenly spaced between -0.05 and -0.1 [1/s]. As k is increased towards infinity, the poles which stay finite approach the zeros of $g(s)$ – which are the values of s where $g(s) = 0$. These are marked with the symbol 'o' on the Nyquist plot, and we see that they lie almost in a circular arrangement around the poles. Importantly, the discretized reactor model has 5 right half plane (RHP) zeros which will "pull" the eigenvalues towards instability as k is increased. As expected, instability occurs for $k = 0.629$ (its nominal value) as the pair of complex RHP-poles closest to the real axis cross into the right half plane.

5.2 Frequency domain analysis

The stability of the system may be analyzed using the standard Nyquist criterion:

> *For a **positive feedback** system with a stable loop transfer function $g(s)k$, the system is unstable if and only if a plot of the loop transfer function $g(j\omega)k$ encircles the $+1$ point (not -1 point) in the complex plane as the frequency ω is varied from $-\infty$ to $+\infty$ (or, equivalently, it is unstable if $g(j\omega)$ encircles the $1/k$ point).*

Consider first the stability of the middle operating point in Figure 5 (for which we show no Nyquist plot). Here, the steady-state loop gain $g(0)k$, the ratio between the two slopes in Figure 5, is larger than 1. Thus, encirclement of $g(j\omega)k$ of the the 1-point is unavoidable, and it follows from the Nyquist stability criterion that the
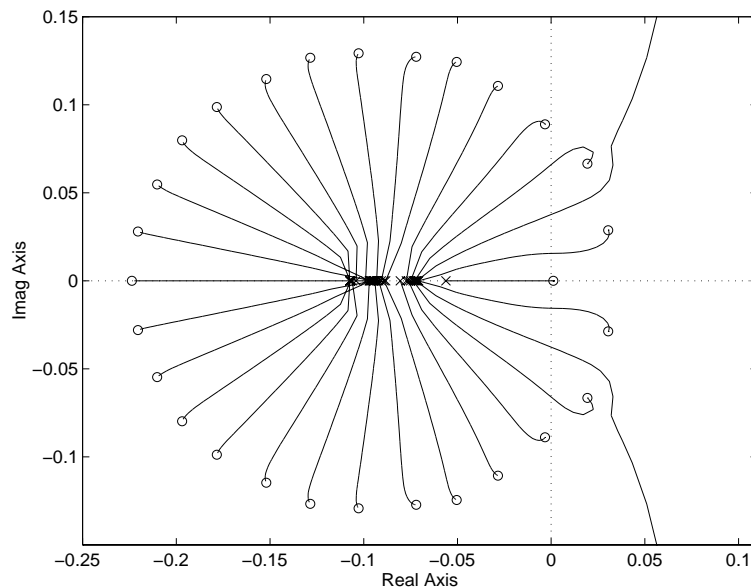

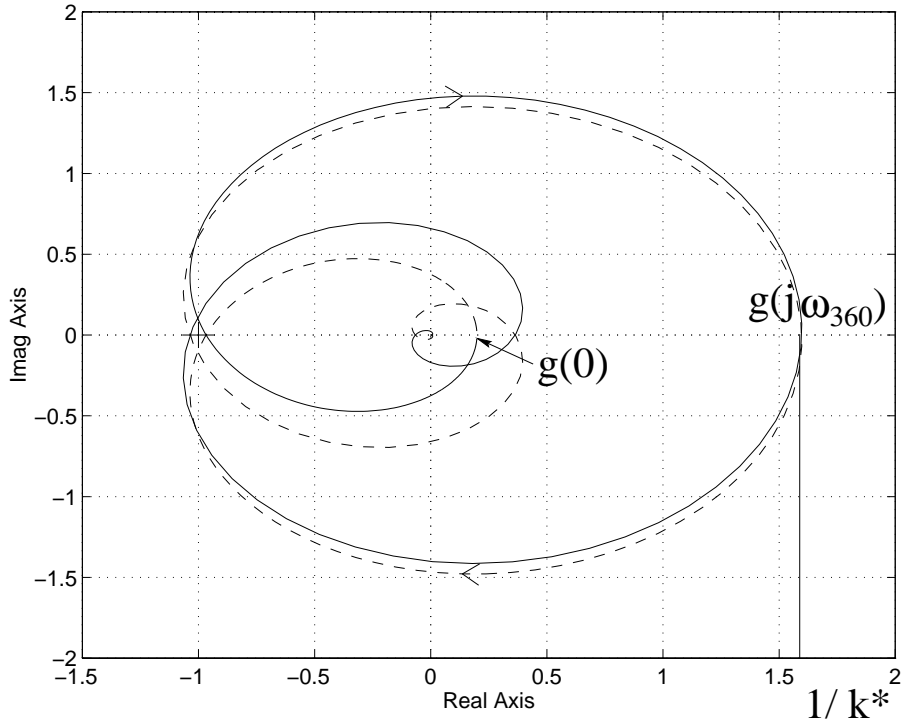Figure 8: Root locus plot of system.

11

Figure 9: Nyquist plot of reactor model $g(s)$.

system is unstable at the middle operating point. This rigorously proves the claim by van Heerden (1953).

Next, consider the stability of the upper (desired) operating point. Normally, one would expect this point to be stable since,

(i) the steady-state loop gain $g(0)k$ is *less* than 1 (it is $0.218 \cdot 0.629 = 0.137$ in our case), and

(ii) the gain $|g(j\omega)k|$ normally decreases with frequency so that instability cannot occur at higher frequencies.

However, in our case there are right half plane (RHP) zeros in $g(s)$ which increase the loop gain and at the same time yield a negative phase shift (see the Bode plot of $g(s)$ in Figure 10), and assumption (ii) is invalid. This is also seen from the Nyquist plot of $g(j\omega)$ in Figure 9, where $g(j\omega)$ is seen to cross the real axis to the right of $g(0)$ at some frequency ω_{360}. The Nyquist stability condition tells that the system will be unstable if this curve encircles the point $1/k$. Thus, the system is stable for small values of k (corresponding to little heat integration), and is unstable if $k > k^*$, where the critical gain k^* is $1/g(j\omega_{360})$. In our case, $k^* = 1/g(j\omega_{360}) = 0.629$ and the preheater gain is $k = \varepsilon = 0.629$, so as expected the system is at its limit to instability at $p = 172$ bar. (For $p = 170$ bar we find $k^* = 1/g(j\omega_{360}) = 0.591$ and the system is unstable). The fact that the instability occurs at a nonzero frequency, also shows that the onset of the instability corresponds to a Hopf bifurcation, which is consistent with the observed limit cycles in the nonlinear simulations.
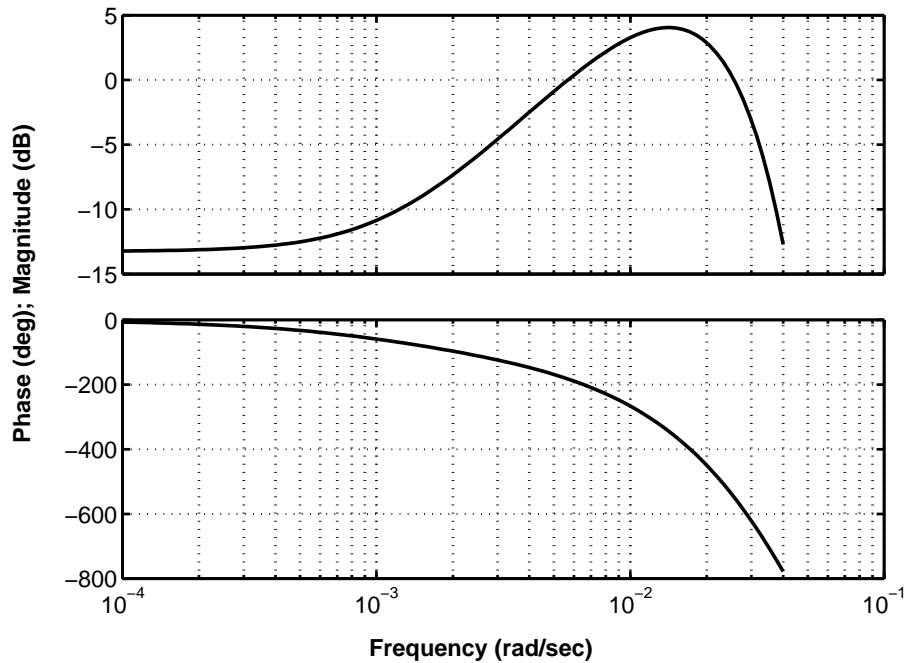
Figure 10: Bode plot of reactor model $g(s)$.

5.3   Step response analysis

We already know that the transfer function of $g(s)$ has several RHP (right half plane) zeros. Such RHP-zeros generally correspond to inverse response behavior, and this is confirmed by Figure 11 which shows the outlet reactor temperature, T_o, in response to a unit step increase in the inlet temperature, $\Delta T_i = 1^\circ C$. The above response is for the linear model, and similar responses were found for the nonlinear model. From the step response we also see that the steady-state gain is about 0.22 as was observed in the Nyquist plot.

The reason why the reactor instability manifests itself as oscillations – and not the more common extinction of the reaction – is this inverse response behavior. A physical explanation for this inverse response is therefore of interest.

Consider a fixed bed where an exothermic reaction is taking place, and suppose we make a sudden increase in the inlet temperature (step change). This will affect the bed outlet by two mechanisms: by the migration of the temperature wave through the reactor, which is a slow process; and by changes in the concentration of chemical species, which is a fast process. The initial effect of the increase in inlet temperature is an increase in the temperature and thus of the reaction rate in the first part of the first bed. This depletes reactant so that the concentration of reactants drops in the last part of the reactor (this effect is fast since the component holdup is negligible), and this causes the reactor outlet temperature to start dropping. However, eventually the
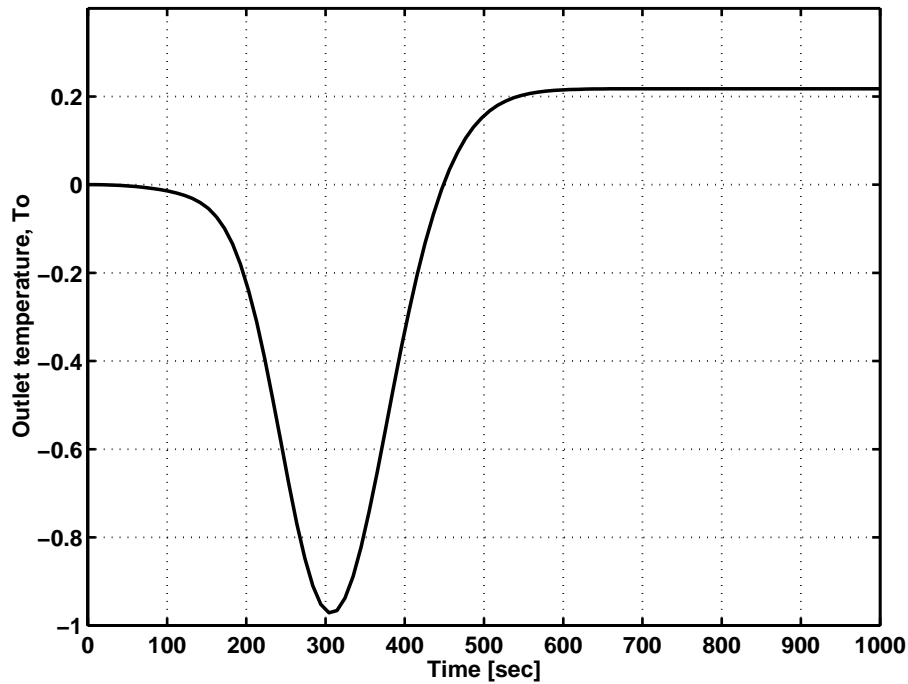
13

Figure 11: Step response of $g(s)$ (Response in T_o to $\Delta T_i = 1^{\circ}C$ for reactor without preheating).

temperature wave moves through the reactor, and the outlet temperature eventually increases. Such inverse response characteristics are well known for chemical reactors (e.g. Silverstein and Shinnar, 1982).

The inverse response behavior corresponds to a frequency response where the gain and phase lag both increase with frequency, and this causes the Nyquist plot to cross the real axis further from the origin at the higher frequency where the phase lag is 360° than at steady-state.

6 Discussion

6.1 Control of reactors with heat integration

Although there has been a lot of work on the control of fixed bed reactors, many reactors in the industry are left uncontrolled. When a processing unit can be operated safely and effectively without control, this is preferred, as it is desirable to keep the complexity of a plant to a minimum.

Two important issues which have to be considered for the ammonia synthesis reactor in question are extinction and limit cycle behavior. Extinction of the reactor—which corresponds to operation at the lower operating point in Figure 5—may occur if the reactor temperature becomes sufficiently low. When this happens, the reactor can not resume normal operation without external addition of heat, which necessitates special

14

startup procedures. Second, the limit cycle behavior, studied in this paper, may lead to damage to the reactor as well as deterioration of the catalyst.

Even a very simple controller may stabilize the reactor system and eliminate the possibility of extinction and limit cycle behavior. For example, consider using the quench valve before the first bed to control the temperature at the first bed inlet. This may be done using a simple PI-controller. This is a simple mixing process with no inverse response so this control loop may be made fast (compared to the overall reactor response time of about 7 min). Thus, the feedback path through the controller will dominate compared with the positive feedback through the preheater, and thus the reactor with controller will behave almost as a reactor without feed-effluent heat exchange. That is, the reactor will exhibit a dynamic behavior similar to a reactor with an independent preheater. To control more carefully the conditions (e.g. temperature) inside the reactor, one could then adjust the setpoint for the inlet temperature in a cascaded manner.

Of course, care must be taken not to saturate the quench valve used for control. For example, if the quench valve becomes fully closed, then there is no further possibility to increase the temperature, and it is likely that the reactor will extinguish. To avoid this, one must increase the heat recovery by reducing the other quench flows such that more of the feed is preheated. This can only be done to a limited extent, so one may instead need to increase the feed temperature, T_f, or increase the reactor pressure.

One may ask whether the observed inverse response (RHP-zeros) through the reactor will limit the performance of the reactor. The answer is most likely "no". The reason is that the inverse response only poses a limitation if one wants to control the reactor outlet temperature T_o (or some other internal temperature in the reactor) using a quench further upstream in the reactor. Most likely, it is not critical that the outlet temperature is tightly controlled, and the RHP-zeros will not present a serious limitation. Also, as already noted, there is no RHP-zero when controlling the inlet temperature using the inlet quench, so stabilization is not limited by RHP zeros.

6.2 Positive feedback

In the Nyquist plot analysis above, it was shown that the reason for oscillatory instability in the ammonia synthesis reactor could be attributed to the shape of the reactor transfer function, $g(j\omega)$. The plot of this transfer function crosses the real axis at a point, $g(j\omega_{360})$, to **the right** of the steady state point, $g(0)$.

However, for most chemical engineering systems, there is no such point of $g(j\omega)$ crossing the real axis to the right of $g(0)$. In such cases, when the positive feedback gain k is increased, the instability occurs as a pole moves through the origin, at which point the presence of the integrator makes the response becomes "slow" and sensitive to disturbances. This has made many authors make statements like: "Positive feedback in a plant makes the response of the plant slow, and the sensitivity to slow disturbances high". Since there are systems where this is not the case, as demonstrated above, such statements should be used with care.

6.3 Comparison with previous work

That ammonia synthesis reactors may exhibit limit cycle behavior, has also been noted by Stephens and Richards (1973); possibly because of an incident in an ICI plant. However, their paper does not contain any dynamic analysis, and it leaves the impression that the authors were somewhat uncertain about the cause of the problem.

On the other hand, the general paper by Silverstein and Shinnar (1982) contains a generic analysis of reactor systems with feed-effluent heat exchange and a combustion chamber. In their analysis, which is based on linear systems theory, they explain the conditions for reactor stability.

7 Conclusion/Summary

An industrial fixed bed autothermal ammonia synthesis reactor became unstable, such that the recorded temperatures in the reactor oscillated heavily. A nonlinear dynamic mathematical model of the reactor reproduces the incident. The oscillatory behavior (limit cycles) occurs in the simulations when the reactor feed temperature or the operating pressure is too low. The phenomena may be described as a temperature wave migrating through the reactor, being fed back through the preheater.

A linear analysis, using Nyquist and Bode plots, can be used to predict the point of instability, and shows that the phenomena occurs when a pair of complex eigenvalues cross into the right half plane. The analysis shows that the physical cause for this somewhat unusual instability, is a combination of the positive heat feedback in the preheater, combined with non-minimum phase behavior (inverse response dynamics) of the reactor temperature response. Thus, the system may become unstable even though there is a positive "stability margin" at steady-state.

The classical steady-state stability analysis of van Heerden (1953) can be used to conclude that the intermediate steady-state is unstable, but not – as illustrated by the results in this paper – to conclude that the upper (desired) steady-state is stable. In any case, it is important to note that any of these steady-states may be stabilized with feedback control.

In the industrial plant, the information obtained from the analysis was used to change the operating procedures to make it less likely for instability to occur. An alternative, and most likely better, solution would have been to implement a feedback control system, but the operators and plant management prefer manual operation. The feedback system could for example use the quench to the first bed to control the temperature at the inlet to the first bed.

Acknowledgement

Additional information

The Matlab and Fortran files for generating the results in this paper and the Ph.D. thesis of Morud (1995) are available over the internet; see the home page of Sigurd Skogestad at `www.chembio.ntnu.no/users/skoge`.

References

[] Aris, R. and Amundson, N.R. (1958). An analysis of chemical reactor stability and control. Ch.Eng.Sci, vol 7, pp 121-155

[] Crider, J.E. and Foss, A.S. (1966). Computational studies of transients in packed tubular reactors. AIChE J., vol. 12, pp 514-522

[] Crider, J.E. and Foss, A.S. (1968). An analytic solution for the dynamics of a packed adiabatic chemical reactor. AIChE J., vol. 14, pp 77-84

[] Eigenberger, G. (1976). *Chem. Eng. Sci.*, vol. 31, pp. 681-.

[] Eigenberger, G. (1985). Dynamics and stability of chemical engng. processes. Int. Chem. Eng. vol. 25, pp. 595-610.

[] Eigenberger, G. and Schuler, H. (1989). Reactor stability and safe reaction engineering. Int. Chem. Eng , vol. 29, pp 12-25

[] Foss, A.S., Edmunds, J.M and Kouvaritakis, B. (1980). Multivariable control system for two-bed reactors by the characteristic locus method. Ind. Eng. Chem. Fundam., vol. 19, pp 109-117

[] Froment, G.F. and Bischoff, K.B. "Chemical Reactor Analysis and Design". 2nd ed., Wiley, New York, 1990.

[] Gusciora, P.H. and Foss, A.S. (1989). Detecting and avoiding unstable operation of autothermal reactors. AIChE J. vol 35, pp 881-890

[] Jørgensen, S.B. (1986). Fixed Bed Reactors and Control - a review. IFAC Symposium DYCORD-86, pp 11-21.

[] Morud, J., *Studies of the dynamics and operation of integrated plants*, Dr. Ing. thesis, Norwegian University of Science and Technology, 1995 (available over the internet).

[] Naess, L., Mjaavatten, A. and Lie, J.O. (1992) Using Dynamic Process Simulation from Conception to Normal Operation of Process Plants. Comp. Chem. Eng., vol 17, no 5/6, pp 585-600

[] Pareja, G. and Reilly, M.J. (1969). Dynamic Effects of Recycle Elements in Tubular Reactor Systems. IEC Fund., vol. 8, 442.

[] Reilly M.J. and Schmitz, R.A. (1966) AIChE J., vol. 12, 153.

[] Reilly M.J. and Schmitz, R.. (1967) AIChE J., vol. 13, 519.

[] Ray, W.H (1972). *2nd ISCRE Symposium*, Amsterdam, pp. A8.1 - A8.19.

[] Schmitz, R.A. (1975). Multiplicity, stability and sensitivity if states in chemically reacting systems - A review. *Advan. Chem. Ser.*, **148**, 156-211.

[] Silverstein, J.L. and Shinnar, R. (1982). Effect of design on the stability and control of fixed bed reactors with heat feedback. Ind. Eng. Chem. Process Des. Dev., vol. 21, pp 241-256

[] Stephens, A.D. and Richards, R.J. (1973). Steady State and Dynamic Analysis of an Ammonia Synthesis Plant. Automatica, vol. 9, pp 65-78

[] Vakil, H.B. *et al.* (1973). Fixed bed reactor control with state estimation. Ind. Eng. Chem. Fund. , vol.12, pp 328-335

[] van Heerden, C. (1953). Autothermic Processes. Properties and Reactor design. Industr. Engng. Chem. (Industr.), , vol.45, 1242

[] Wallmann, P.H. and Foss, A.S. (1979). Multivariable integral control for fixed bed reactors. Ind. Eng. Chem. Fund. , vol.18, pp 392-399

[] Wallmann, P.H. and Foss, A.S. (1981). Experiences with dynamic estimators for fixed bed reactors. Ind. Eng. Chem. Fund. , vol.20,pp 234-239

Appendix. Data for the model

The reaction is $N_2 + 3H_2 \rightleftharpoons 2NH_3$.

Gas heat capacity, C_{pg}	$3500 \ J/kg, K$
Heat capacity of catalyst, C_{pc}	$1100 \ J/kg, K$
Heat of reaction $-\Delta H_{rx}$	$2.7 \cdot 10^6 \ J/kg \ NH_3$

Volume, bed 1	$6.69 \ m^3$
Volume, bed 2	$9.63 \ m^3$
Volume, bed 3	$15.2 \ m^3$
Catalyst bulk density, ρ_{cat}	$2200 \ kg/m^3$
Typical gas density	$50 \ kg/m^3$
Dispersion coefficient, bed 1, , $_1$	$5.6 \cdot 10^{-4} \ (bed \ lenghts)^2/sec.$
Dispersion coefficient, bed 2, , $_2$	$4.6 \cdot 10^{-4} \ (bed \ lenghts)^2/sec.$
Dispersion coefficient, bed 3, , $_3$	$3.3 \cdot 10^{-4} \ (bed \ lenghts)^2/sec.$
Number of discretization points in each bed	10

Operating conditions:

Inlet flow to preheater, w_h	$127 \ tons/hr$
Quench bed 1, w_{Q1}	$58 \ tons/hr$
Quench bed 2, w_{Q2}	$35 \ tons/hr$
Quench bed 3, w_{Q3}	$32 \ tons/hr$

Feed mole fraction NH_3	0.0417
Feed mole fraction N_2	0.2396
Feed mole fraction H_2	0.7187
Feed gas temperature, T_f	$250 \ ^\circ C$
Typical reactor pressure	$200 \ bar$

Preheater:

Heat transfer coefficient, U	$536 \ W/m^2, K$
Heat exchanger area, A	$283 \ m^2$
Calculated number of heat transfer units, NTU	1.23
Calculated heat exchanger efficiency, ϵ	0.629

$$\varepsilon = \frac{1 - e^{-NTU(1-C)}}{1 - Ce^{-NTU(1-C)}}$$

where

$$NTU = \frac{UA}{w_h C_{pg}}, \quad C = \frac{w_h}{w_h + w_{Q1} + w_{Q2} + w_{Q3}}$$

1   2   3